

A Dark Energy Figure of Merit in Higher Dimensions

Andreas Albrecht

Department of Physics, University of California at Davis, One Shields Avenue, Davis, CA 9561

Gary Bernstein

Department of Physics & Astronomy, University of Pennsylvania, 209 S. 33rd St., Philadelphia, PA 19104

(Dated: August 13, 2006)

We consider a nine-dimensional parameterization of the dark energy equation of state and compare this with the two-dimensional analysis recently used by the Dark Energy Task Force (DETF) to compare the constraining power of various experimental approaches. We extend the figure of merit analysis used by the DETF to our parameterization and apply it to the DETF data models. The data models constrain 3-4 of our parameters just as well as they constrain the two DETF parameters. While supporting most of the DETF conclusions, our results point to a much higher impact for the larger dark energy experiments than was reported by the DETF. Most of our differences from the DETF can be understood using a simple dimensional rescaling formula.

PACS numbers: Valid PACS appear here

The observed cosmic acceleration requires the introduction of the “dark energy” to achieve consistency with the current cosmological paradigm. The dark energy must be the dominant component of the universe (about 70% of the energy density), yet an understanding of its fundamental nature has proved elusive. Many believe that resolving the mystery of the dark energy will force a radical change in our understand of fundamental physics. This expectation has generated great interest in the dark energy and widespread enthusiasm for an aggressive observational program to help resolve the mystery.

Recently, the Dark Energy Task Force (DETF)[1] released a report to guide the planning of future dark energy observations. The DETF used a dark energy “figure of merit” (FoM) based on a two-parameter description of the dark energy evolution in order to produce quantitative findings. An interesting question is whether using the DETF FoM might lead to poor choices in shaping an observational program because of its simplicity. In particular, could the relative value of two possible experiments be distorted by the DETF FoM?

This paper considers this question by examining an alternative FoM. We model the dark energy evolution with a nine-parameter model and formulate a FoM (the “D9 FoM”) which gives an experiment credit for any combination of these parameters which it constrains well. We’ve used this alternative FoM to assess many of the same simulated data sets considered by the DETF.

Our analysis leads to three main conclusions: 1) In our scheme, most of the DETF data models measure significantly more than two parameters to useful accuracy. 2) The main differences between our results and the DETF results can be accounted for by a simple dimensional rescaling reflecting the increased parameter space. 3) Due to the reduced dimensionality, the DETF FoM significantly understates the relative importance of the different experimental stages, as compared with the 9D FoM. In particular, the 9D FoM indicates a much greater impact from larger Stage 4 projects as compared with

that reported by the DETF. Our FoM gives the similar relative rankings of data models and combinations of data models as found by the DETF. We find no evidence for any major distortion of the DETF conclusions beyond this overall rescaling.

Following the DETF (and many others) we model the dark energy as a homogeneous and isotropic fluid. The complete dark energy history can then be given by the dark energy density today and the “equation of state parameter” (the ratio of the density and pressure of the fluid) $w(a)$ as a function of time or cosmic scale factor a .

The key to our discussion of FoM’s is the choice of parameterization of $w(a)$. The DETF used a standard linear form

$$w(a) = w_0 + w_a(1 - a) \quad (1)$$

For this work we used a piecewise constant model of $w(a)$

$$w(a) = -1 + \sum_i w_i T(a_i, a_{i+1}) \quad (2)$$

where the “tophat function” $T(a_1, a_2)$ is unity for $a_1 > a \geq a_2$ and zero otherwise. In this parameterization any non-zero value of a w_i represents a deviation from a cosmological constant ($w = -1$). Note that the DETF linear model is well approximated by a subspace of the nine-dimensional model.

The DETF considered a variety of data models and calculated the degree to which w_0 and w_a would be constrained by each data model. The DETF FoM is given by the reciprocal area in $w_0 - w_a$ space enclosed by the 95% confidence contour for a given data model. Our “9D” figure of merit is defined as the reciprocal hyper-volume in the nine dimensional space enclosed by the 95% confidence contour for a given data model.

Like the DETF we use the Fisher matrix formalism and assume a Gaussian probability distribution to evaluate the 9D FoM. A general (unnormalized) Gaussian

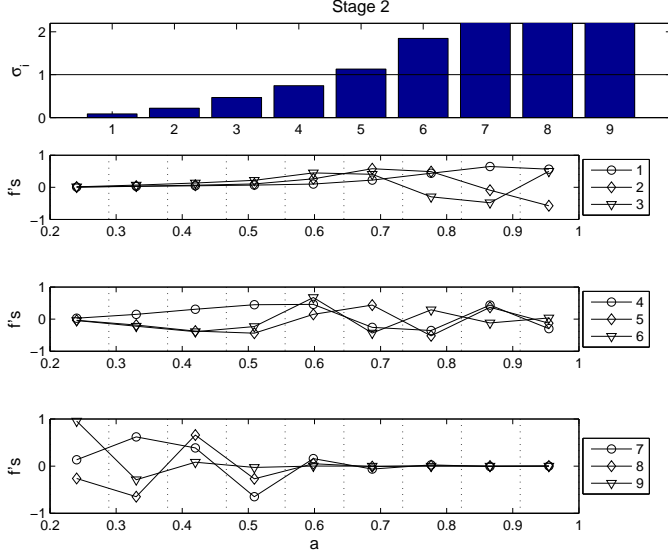


FIG. 1: Information about \mathbf{F} for the DETF Stage 2 data model. The upper panel gives the errors σ_i (in order of increasing σ_i), and lower panels give the corresponding eigenvectors \vec{f}_i . The \vec{f}_i represent the independently measured “modes” of $w(a)$. The plot shows the nine components of each \vec{f}_i with markers (assigned to each eigenmode i according to the legend) giving all nine parameter values w_j as a function of step label $\bar{a}_j \equiv \sqrt{a_j a_{j+1}}$ for that vector. The dotted vertical lines show the values of a_j .

probability distribution for parameters \vec{x} around a central value \vec{x}_0 in N dimensions is given by

$$\exp(-\Delta\vec{x}\mathbf{F}\Delta\vec{x})/2 \quad (3)$$

were $\Delta\vec{x} = \vec{x} - \vec{x}_0$. The N eigenvectors \vec{f}_i of \mathbf{F} give the directions of the principle axes of the error ellipsoid, and the width of the error ellipsoid along axis \vec{f}_i is given by σ_i , the inverse square root of the i -th eigenvalue of \mathbf{F} .

Note that any given function $w(a)$ parameterized by Eqn. 2 is uniquely specified by the vector \vec{w} with components $\{w_i\}$. The vectors \vec{f}_i form an orthonormal basis that spans the space of all possible \vec{w} 's, and thus any function $w(a)$ in this parametrization can be specified by coefficients α_i so that $\vec{w} = \sum_i \alpha_i \vec{f}_i$. The data corresponding to \mathbf{F} make uncorrelated measurements of the α_i 's with errors given by σ_i .

Our FoM is proportional to $\prod_i \sigma_i^{-1}$ (the constant of proportionality is irrelevant to our discussion since only ratios of FoM's are discussed). The only formal difference between the DETF and 9D FoM's is the parameter space in which they are defined. For this work we calculate 9D FoM's for a wide range of DETF data models, but we exclude DETF models of galaxy cluster data because these data models are too complex to easily adapt to our scheme.

Each data model corresponds to its own Fisher matrix \mathbf{F} from which the FoM can be calculated. Figure

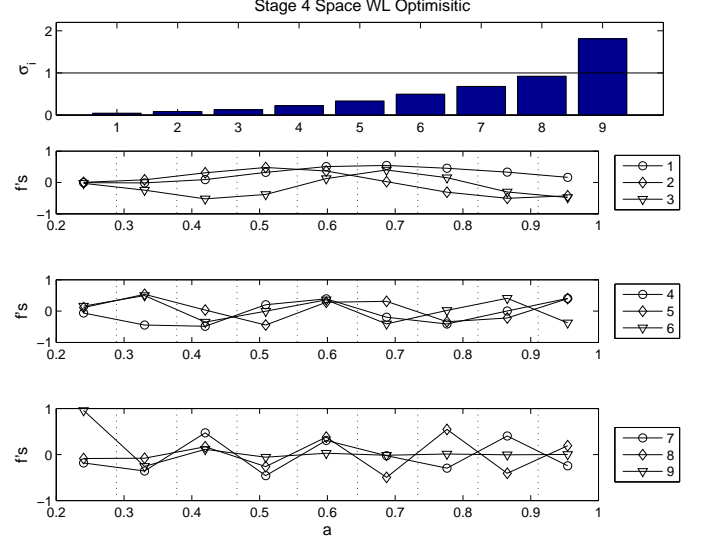


FIG. 2: This figure has the same format as Fig. 1, only this one shows information about the DETF “Stage 4 Space Weak Lensing Optimistic” data model. Note that more modes are well measured for this much higher quality data set (vs Stage 2).

1 gives information about the \mathbf{F} corresponding to the DETF “Stage 2” data minus clusters. This is the DETF projection of where we will be when current projects are complete. The upper panel shows the σ_i 's, (sorted by increasing size) and the lower panels show the corresponding eigenvectors of \mathbf{F} as a function of a . Figure 2 gives the same information for a particular Stage 4 data model. None of the DETF data models are powerful enough to constrain all nine directions in our parameter space. This is reflected in very large values of σ_i for larger i .

All the 9D FoM's reported here used a model of $w(a)$ where the grid on which the constant pieces of $w(a)$ are defined starts at $z_{min} \equiv 1/(a_{min} - 1) = 0.01$ and goes out to $z_{max} = 4$. The bins are evenly spaced linearly in a . For this work we also considered bins evenly spaced logarithmically in a as well as both types of spacing in z as well. For each of these cases we also considered grids with $z_{max} = 2$ and $z_{max} = 7$. The grid used for the results reported here is the one (out of all of these examples) which gives the highest FoM's. That way we use the parameters which are best measured by the model data sets.

We choose to not attach significance to the poorly determined directions (directions with large σ_i). We do not trust our formalism to give meaningful answers in directions that place bounds weaker than unity on the w_i 's, and such weak constraints are not likely to enlighten us about dark energy. We handle this issue by re-setting all $\sigma_i > 1$ to unity when we calculate the FoM. That way changes in σ_i in the directions where the method is not trusted do not contribute to changes in the FoM.

This stepwise constant form for $w(a)$ has been used

previously by other authors (applied to different data models)[2, 3, 4]. To the extent that comparison is possible our work is consistent with these earlier papers. In particular, the claims in [4] that there are only two measurable w parameters stems from a different formal definition of what it means to measure a parameter usefully. The choice we make here is best suited for to our purpose, which is to make a direct comparison with the DETF methods.

The DETF present their main results in four bar charts showing the FoM ranges for particular data models. The values are given as ratios to the Stage 2 FoM so that progress beyond Stage 2 can be read directly, with increasing progress corresponding to larger values along the y-axis. The four panels in Fig. 3 show equivalent plots (using the same DETF data models minus clusters). The dark bars show the DETF FoM and the light bars show the 9D FoM. The 9D FoM shows much larger values for all the strong data models.

Aside from not including clusters, there are other small differences between the data models used here vs those used for the DETF plots. When we use two supernova data models in combination, such as when stage 2 and stage 3 or 4 data are combined, they share the same nuisance parameters (except for the photometric redshifts). In the DETF calculations the nuisance parameters are separate. The PLANCK prior is calculated the same way as for DETF, but the Fisher matrix is expressed in the variables $\{n_s, \delta_\zeta, \omega_m, \omega_b, \theta_s\}$ where we use $\ln(\theta_s) = -0.252\ln(\omega_m) - 0.83\ln(\omega_b) - \ln(D_A^{\text{co}}(a^*)) + 8.2094$ (from Eqn. (23) in [5]) These parameters are defined in the DETF report. Also, the calculations here apply the transfer function formalism for weak lensing in a manner that is formally equivalent but different in implementation. This exposes the shortcomings of the transfer function formalism as discussed in section 9.2 of the DETF technical appendix which results in FoM's slightly differently than those published in the DETF report. These small difference from the DETF report were included in all the FoM's presented here so comparisons between DETF and 9D will just reflect the different parameters choices.

One can see that good combinations of Stage 3 data give 9D FoM improvements of an order of magnitude and strong Stage 4 data combinations give 9D FoM improvements of three orders of magnitude or more. Compared with the DETF results (about an order of magnitude to Stage 4 and half an order of magnitude to Stage 3) this is not only a strong showing overall, but specifically the 9D FoM exhibits a greater improvement factor going from Stage 3 to Stage 4 as compared with the DETF FoM.

One can explore the relationship between the 9D and DETF FoM's by considering the parameter space dimensionality. The DETF FoM is constructed in a 2-D parameter space. Consider the following effective “reduction to 2-D” of the 9D FoM:

$$\mathcal{F}_2 \equiv \mathcal{F}_9^{2/D_e} \quad (4)$$

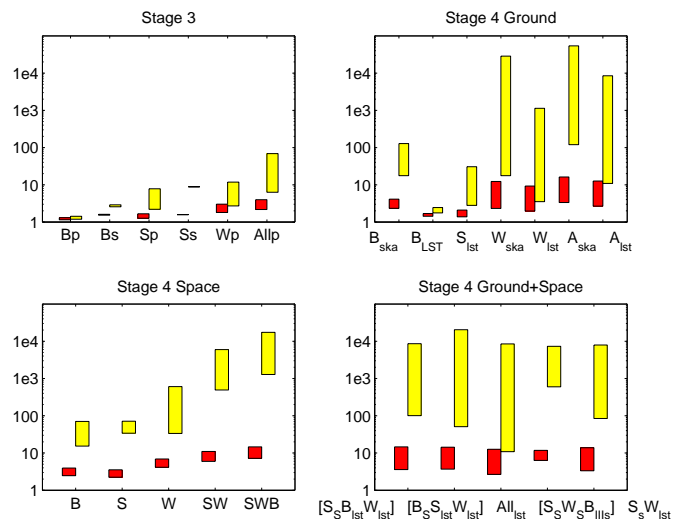


FIG. 3: Each of the four panels shows a plot that corresponds to one of the four main bar charts in the DETF report (having the same titles). The data models are essentially the same as those used by the DETF and, as with the DETF plots, the bars show improvement in the FoM over Stage 2. The dark bars show the DETF FoM. To the right of each dark bar is a light bar that reflects the 9D FoM for the identical data model. The 9D FoM registers a much greater impact from each data model, and also a much greater improvement Stage 4 vs Stage 3. The x-axis labels are similar to those on the DETF plots, but abbreviated.

Here \mathcal{F}_2 and \mathcal{F}_9 are the reduced and regular 9D FoM's respectively. This dimensional reduction basically means that \mathcal{F}_2 is the product of only two $1/\sigma_{\text{eff}}$'s where σ_{eff} is a suitably defined geometric mean of the σ_i 's. The “effective dimension” D_e should be thought of as the number of directions constrained by a given data model in 9D parameter space.

Figure 4 shows the same plots as in Fig 3 except Eqn. 4 has been applied to all the 9D FoM's as described in the figure caption. The rough agreement between the DETF and reduced 9D bars in Fig 4 suggests that rescaling according to Eqn.4 accounts for the major differences between the 9D and DETF FoM's.

Imposing additional constraints or “priors” on specific parameters generally will improve the figures of merit. The DETF report has a plot similar to Fig. 5 (dark bars) which illustrates the “impact factor” (factor by which the FoM improves) of imposing stronger priors on the curvature and the Hubble constant. DETF found the impact to be modest, and noted that the best data models actually determine these (and other) parameters so well themselves that the impact of additional priors was in fact very small.

Here we have shown how data models can constrain more $w(a)$ parameters than the two considered by the DETF. Does this improvement comes at the expense of poorer constraints on other parameters, due to the greater flexibility of the dark-energy model? The lighter

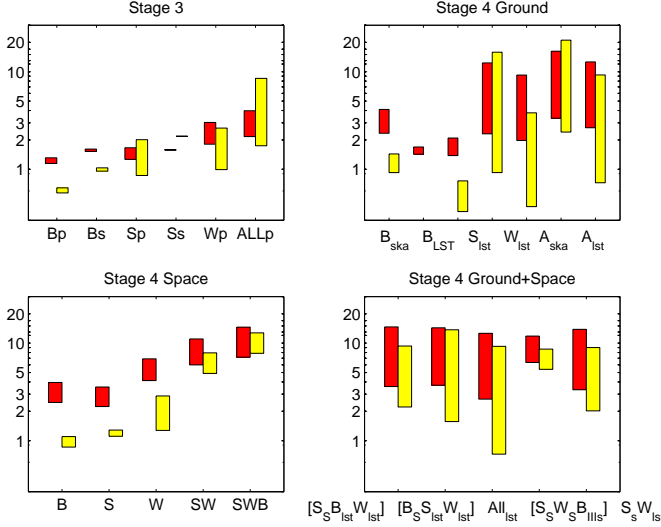


FIG. 4: This plot has the same form as Fig. 3, except here all the 9D FoM’s have been scaled according to Eqn. 4. We use $D_e = 2.5$ for Stage 2, $D_e = 3$ for Stage 3, $D_e = 4$ for Stage 4 pessimistic and $D_e = 4.5$ for Stage 4 optimistic. These plots suggest that the scaling accounts for most substantial differences between the two FoM’s exhibited in Fig. 3. We probably have somewhat overestimated D_e for some of the weaker data models (leading to lower 9D bars), and even accounting for that, some modest differences may remain.

bars in Fig. 5 show the impact factor on the 9D FoM. The impact factors are broadly the same for both the 9D and DETF FoM’s, indicating that going to the 9 parameter $w(a)$ model does not produce significant degradation of the impact of the data models on these two parameters. In fact, the 9D impact factors are smaller with the Hubble prior than for the DETF FoM, suggesting that the 9D space allows the data to prove its worth on other $w(a)$ parameters which have even less degeneracy with the Hubble parameters than w_0 and w_a .

We have analyzed a figure of merit for dark energy data models defined in a nine-dimensional parameter space, up from the two-parameter space used by the DETF. Our 9D FoM allows a given data model more leeway to show its capabilities, since there are many more directions in parameter space that it might constrain well. We have found that the DETF data models constrain more parameters than the two used by the DETF. Specifically, our scaling law indicates that stage 3 data models constrain on average 3 parameters with the same uncertainties as they constrain the two DETF parameters, and the stage 4 data models constrain four or more parameters with the same average uncertainties as they constrain the two DETF parameters.

Our 9D FoM follows the same logic as the DETF FoM, namely it attaches equal weight to any constraint on $w(a)$. For example, the measurement of a non-zero value for any of the α_i ’s (that is any of the independently measured combinations of the w_i ’s) *would* be equally signif-

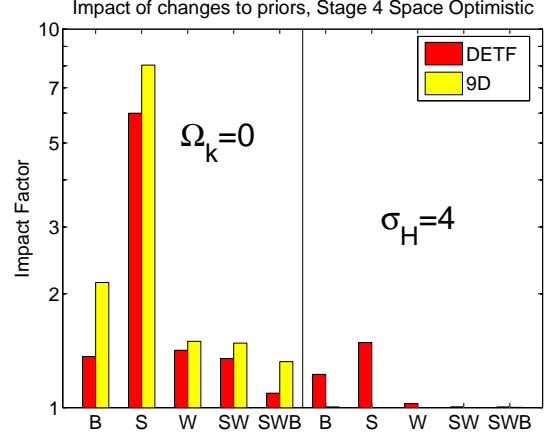


FIG. 5: This plot shows the impact on the FoM of adding additional constraints on curvature (left side) and the Hubble constant (right side). Although the format is different, the details are the same as the corresponding plot in the DETF report. The dark bars show the impact on the DETF FoM and the light bars show the impact on the 9D FoM. Specifically, the plotted “impact factor” is the factor by which the FoM’s change (for Stage 4 space, without stage 2) when the additional priors are imposed. The results are similar for both FoM’s.

icant in that it would rule out a pure cosmological constant. Thus the higher dimensional constraints really do reflect greater discovery power.

Because our calculations allow the different data models to show their capabilities to constrain $w(a)$ in larger parameters spaces our 9D FoM’s are much larger overall, especially for the powerful stage 4 data models. By modeling $w(a)$ with only two parameters one could argue that the DETF FoM underestimates the overall impact of the DETF data models. Especially, the DETF FoM underestimates the relative value of “Stage 4” (large projects) vs “Stage 3” (medium projects). The basis for most of the 9D-DETF differences can be understood in terms of a simple rescaling of the 9D results according to Eqn. 4. The 9D FoM gives broadly the same relative rankings of data models and combinations of data models as found by the DETF. Thus, aside from overall rescaling that gives much more credit to the larger experiments, our calculations broadly support the DETF conclusions, especially regarding the value of combining methods and the relative rankings of specific data models.

Acknowledgments

We thank all the DETF members for a great collaboration which formed the basis of this work. We also thank Lloyd Knox for providing our simulated PLANCK Fisher matrices and for helpful discussions. This work was supported in part by DOE grants DE-FG03-91ER40674 (AA) and DE-FG02-95ER40893 (GB) and by NASA

grant NASA BEFS-04-0014-0018 (GB).

-
- [1] The DETF report can be found at www.nsf.gov/mps/ast/detf.jsp. It will soon be posted on the ArXiv.
- [2] D. Huterer and G. Starkman, Phys. Rev. Lett. **90**, 031301 (2003), astro-ph/0207517.
- [3] L. Knox, A. Albrecht, and Y. S. Song (2004), astro-ph/0408141.
- [4] E. V. Linder and D. Huterer, Phys. Rev. **D72**, 043509 (2005), astro-ph/0505330.
- [5] W. Hu, ASP Conf. Ser. **399**, 215 (2005), astro-ph/0407158.